The Journal of Engineering Research Vol. 4, No.1 (2007) 23-36

Direct Design of T-Beams for Combined Load of Bending and Torsion

A. S. Alnuaimi*, K.S. Al-Jabri and A.W. Hago

Department of Civil and Architectural Engineering, Sultan Qaboos University, P.O. Box 33, Al Khodh 123, Muscat, Oman

Received 22 November 2005; accepted 24 April 2006

التصميم المباشر للجيزان ذوات الشفة المعرضة لاحمال الانحناء والالتواء

علي النعيمي و خليفه الجابري وعبدالواحد هجو

الخلاصة: أجريت الاختبارات على خمسة جيزان من الخرسانة المسلحة ذوات شفة أخضعت لمجموعة احمال مكونة من إنحناء والتواء. وقد تم استخدام حقل اجهاد مطاطي اضافة لمعيار نيلسين ثنائي الابعاد والخاص بخضوع الخرسانة المسلحة المعرضة لتاثير القوى المستوية في طريقة التصميم المباشر للحصول على كميات حديد التسليح. وكانت أبعاد الجيزان كالاتي: عرض الشفة ٦٠٠ مليميتر وسمك الشفة ١٥٠ مليميتر وعرض الوترة ٢٠٠مليميتر والسمك الكلي ٦٠٠ مليميتر وطول الجائز ٥٢٠٠ مليميتر. وتمت مقارنة كميات حديد التسليح المحسوبة بطريقة التصميم المباشر بتلك التي تحسب بواسطة الكودين الامريكي والبريطاني. ووجد ان كميات حديد التسليح في الاتجاه الطولي المحسوبة بطريقة التصميم المباشر تماثل الكميات التي يتطلبها الكود الامريكي لكنها اقل من تلك التي يتطلبها الكود البريطاني. وفي الجهة المستعرضة فإن طريقة التصميم المباشر تتطلب كميات من حديد التسليح اقل بكثير مما يتطلبة الكودان الامريكي و البريطاني. وفي الدراسة الحالية فإن المتغير الرئيسي كان نسبة عزم الالتواء الاقصى الى عزم الانحناء وتضمنت الدراسة قيما متعددة لهذه النسبة بين٠,٦ الى ١,٥ وقد توصلت الدراسة الى عدم وجود اختلافات كبيرة بين احمال التصميم واحمال الانهيار للجيزان التي تمت دراستها كما وجد ان اغلب حديد التسليح في الاتجاه الطولي والمستعرض قد وصل او قارب اجهاد الخضوع عندما تقترب الاحمال من احمال التصميم، كما ان كل الجيزان قد انهارت عند احمال تقترب من احمال التصميم وكانت ذوات سلوك مرن حتى عند انهيارها. وقد خلصت الدراسة الى انة يمكن استعمال طريقة التصميم المباشر في تصميم الجيزان الخرسانية ذوات الشفة والمعرضة لاحمال الانحناء واللتواء.

المفردات المفتاحية: الجيزان ذوات الشفة، طريقة التصميم المباشر، انحناء، اللتواء، الخرسانة المسلحة.

Abstract : Tests were conducted on five reinforced concrete T-beams subjected to combined load of bending and torsion. Elastic stress field in conjunction with Nielsen's 2D yield criterion for reinforced concrete subjected to in-plane forces were used in the Direct Design Method for the design of reinforcement. The beam dimensions were: flange width = 600mm, flange thickness = 150mm, web width = 200mm, total depth = 600mm and beam length = 5.2m. Required reinforcement calculated using the Direct Design Method was compared with the ACI and BSI codes. It was found that the Direct Design Method requires longitudinal reinforcement similar to the ACI code but less than the BSI code. In the transverse direction, the Direct Design Method requires much less reinforcement than both codes. The main variable studied was the ratio of the maximum twisting moment to the bending moment which was varied between 0.6 and 1.5. Good agreement was found between the design and experimental failure loads. Most of the longitudinal and transverse steel yielded or reached near yield stress when the design load was approached. All beams failed near the design loads and undergone ductile behaviour until failure. The results indicate that the Direct Design Method can be successfully used to design reinforced concrete T-beams for the combined effect of bending and torsion loads.

Keywords: T-beams, Direct design method, Bending, Torsion, Reinforced concrete

Notations

A_c	gross area of the whole cross-section
A_o	area of the cross-section enclosed by the shear flow centreline
A_x,A_y	steel areas per unit width in x and y directions respectively
E	Young's modulus of elasticity
f_{cu}	concrete cube compressive strength
f_{sx}	steel stress in the longitudinal direction
f_{sy}	steel stress in the transverse direction

---

*Corresponding author's e-mail: alnuaimi@squ.edu.om

f_y	yield strength of longitudinal steel
f_{yv}	yield strength of transverse steel
I	moment of inertia of the section
L.F.	load factor = $(T_i/T_d + M_i/M_d)/2$ at any load increment *i*
L_e/L_d	failure load ratio = $(T_e/T_d + M_e/M_d)/2$ for the last (failure) load increment
N_1	concrete resisting force in the principal direction 1, $(=\sigma_1 t)$
N_2	concrete resisting force in the principal direction 2, $(=\sigma_2 t)$
N_x	applied in-plane force per unit length in the x direction on a element with thickness *t*, $(=\sigma_x t)$
N_{xy}	applied in-plane shear force per unit length on a element with thickness *t*, $(= \tau_{xy} t)$
N_y	applied in-plane force per unit length in the y direction on a element with thickness *t*, $(=\sigma_y t)$
N^s_y	resisting forces in x direction steel $(= A_x f_{sx})$
N^s_y	resisting forces in y direction steel $(= A_y f_{sy})$
t	thickness of the element
T_d, M_d	design torsion and bending moment respectively
T_e, M_e	experimentally measured torsion and bending moment at failure
T_i, M_i	experimentally measured torsion and bending moment at load increment *i*
y	distance from the neutral axis to the location where stress to be calculated
σ_1	concrete principal stress in direction 1
σ_2	concrete principal stress in direction 2
σ_x, σ_y	applied normal stresses in x and y directions respectively
ε	measured steel strain at any load increment *i*
ε_y	longitudinal steel yield strain $(= f_y/E)$
ε_{yv}	transverse steel yield strain $(= f_{yv}/E)$
τ_{xy}	applied elastic shear stress

1. Introduction

The present code design equations for concrete structures (especially for shear and torsion) are largely based on experimental results which lead to continuous changes in the code. Calculation of reinforcement for each load is done separately and then summed algebraically which leads to conservative design.

For combined loading, several interaction theories based on ultimate strength criterion have been developed (*ie*. theories on Truss-Analogy and Skew-Bending), but the major weakness of this approach lies in the fact that it does not present a general design procedure capable of being applied to design for a given general stress state.

Many researchers investigated the behaviour of reinforced and pre-stressed concrete T-beams under different loading conditions (*ie*. bending, torsion and shear) and the contribution of the sections' elements (*ie*. flange and web) on resisting applied forces has been also reported. The experimental behaviour of twenty six reinforced concrete T-beams without web reinforcement under combined bending, shear and torsion was reported by Farmer and Ferguson, (1967). Torque-to-shear ratios of 1.5, 3 and 6 were investigated. Results indicated that span length and cross-sectional warping was not found to influence the behaviour greatly. It also suggested that torsion lowered the shear strength of the beam much less than ordinary plastic theory would suggest. Nawy and Potyondy (1971) studied the flexural cracking behaviour of pre-tensioned I- and T-beams. They tested twenty two I- and T-beams with a span of 9-ft (2.74m) and pre-stressed with 1/4 in (6.35mm) diameter 7-stranded wires. From the results, it was concluded that the confining reinforcement had no influence on the magnitude of load at first crack and T-sections cracked at a lower load than I-sections. Kirk and Loveland (1972) observed, after testing eighteen unsymmetrical reinforced T-beams under bending and torsion, that the location of longitudinal steel at the top or the bottom of the section can have significant influence on the torsional resistance. The effect of reinforced flanges on the torsional capacity of reinforced concrete T-beams was investigated by Zararis and Penelis, (1986). Eighty two T-beams with various flange widths and percentages of reinforcement were tested in combined torsion and bending. Results showed that there is significant contribution from the reinforced flanges to the torsional capacity of the T-beams especially when torsion prevailed. Experimental studies by Kotsovos *et al*. (1987) also showed that the shear resistance of T-beams with shear-span-to-depth ratios greater than 2.5 is provided by the flange and not as widely accepted by the web. Gurfinkel and Fonseca (1996) investigated the ACI code requirement for additional ductility in the T-beam sections and reported that "There is little justification for code-imposed additional demand on minimum ductility of T-beams sections". Recently experimental investigation was carried out by Rahal and Collins, (2003) in order to evaluate the ACI and AASHTO-LRFD design provisions for combined torsion and shear. It was found that the ACI provisions give very conservative results if the recommended value of 45-degree is used for the inclination of the compression diagonals.

It is clear from the above literature and others that large area of disagreement exists among the researchers on the design of T-beams when shear and torsion are involved. One reason for this disagreement is the fact that the design equations used in the code are not based on sound theoretical principles like the theories of mechanics (*ie*. Theory of Plasticity).

The Direct Design Method, which is based on the Lower Bound Theorem of the Theory of Plasticity, presents a solution to some of the above pitfalls. This procedure satisfies the fundamental requirements of classical Theory of Plasticity (equilibrium condition, yield criterion and mechanism condition) and it reduces the ductility demand assumed for metals. In contrary to the existing codes of practice, this method precludes the use of empirical equations and therefore, it is less vulnerable to changes and may form a basis for a unified design method.

Previous work by Bhatt and Ebireri (1989) had shown that the 'direct design method' could be applied to the design of hollow and solid beams with square cross-section subjected to combined bending and twisting moments. Alnuaimi and Bhatt (2004a, b) used the direct design method for the design of eight reinforced concrete square hollow beams subjected to combined bending, torsion and shear. The main variables studied were the ratio of twisting moment to the bending moment and the ratio of the shear stress due to torsion to the shear stress due to shear force. They concluded that the direct design approach used, gave satisfactory results with beams failing within the range of the design loads and behaving in a ductile manner until failure. Many other researchers have successfully used the direct design method for the design of different types of structures (Kemp 1971; Nielsen 1974; Morley 1977; Memon 1984; El-Nuonu 1985; Hago and Bhatt 1986; Abdel-Hafez 1986; El-Hussein 1994; Bhatt and Bensalem 1996a, b; Bhatt and Mousa 1996; and Elarabi 1999).

In this research, the direct design method was used for the design of five reinforced concrete T-beams. The beams were subjected to combined load of bending and torsion. The required reinforcement obtained using the direct design method was compared with that obtained using the ACI (2002) and the BSI (1997) codes.

2. Research Significance

A Theory of Plasticity-based, design procedure for the design of reinforced concrete T-beams subjected to combined loading of bending and torsion is presented as replacement for the empirical-based methods used by the codes of practice. The required reinforcement from this procedure, Direct Design Method, is compared with the required reinforcement using the ACI and the BSI codes. Test results from five T-beams designed using the direct design method are presented.

3. Test Beams

Five reinforced concrete T-beams were designed for combined action of bending and twisting moments using the direct design method. The beams were 5200 mm long with overall depth of 600 mm. The dimensions of the T-section were 600 x 150 mm flange and 450 x 200 mm web. Table 1 shows loads that each beam was designed to resist. The main variable in this series was the ratio of the design twisting moment to the bending moment, T_d / M_d, which varied between 0.6 and 1.5. Figure 1 shows the geometry and dimensions of the tested beam.

Table 1. Design load combinations

Beam No.	T_d kN.m	M_d kN.m	T_d / M_d Ratio
TB1	36	60	0.60
TB2	75	100	0.75
TB3	50	60	0.83
TB4	72	72	1.00
TB5	108	72	1.50

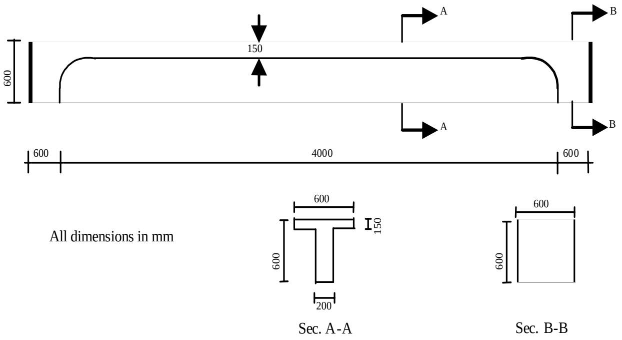

Figure 1. Beam geometry and dimensions

4. Comparison Between the ACI and BSI Codes and the Direct Design Method

Table 2 shows the required reinforcement for the T-beams used in this research based on the ACI and BSI codes and the direct design method, DDM. It can be seen that the direct design approach leads to longitudinal steel requirement close to the ACI code while the BSI code is more conservative. In the transverse reinforcement, the direct design procedure required less reinforcement than both codes in most cases, especially the BSI code. The direct design method was used for the design of this research beams.

5. Design of T-beams

The following steps were used for the design of T-beams, and a numerical example is given in appendix A. Detailed derivation of equations can be found elsewhere Alnuami and Bhatt, (2004a, b).

Table 2. Required reinforcement using the ACI, BSI and DDM methods

Beam No.	ACI		BSI		DDM	
	A_s (mm^2)	A_{sv}(mm^2/m)	A_s (mm^2)	A_{sv}(mm^2/m)	A_s (mm^2)	A_{sv}(mm^2/m)
TB1	1136	914	1325	978	1091	606
TB2	1903	1848	2479	1978	1908	1226
TB3	1484	1269	1746	1358	1516	842
TB4	1841	1741	2457	1956	1932	1155
TB5	2633	2611	3542	2934	2897	1732

1. Calculate the ultimate (factored) design bending moment M_d and torsion T_d at the section based on the loading condition, support locations and geometry of the beam.
2. Divide the cross-section into different levels (regions) as shown in Fig. 2.
3. Find the neutral axis, the moment of inertia and the area enclosed by the shear flow centreline.
4. Calculate normal stress σ_x due to applied load at the centre of each region (level) using elastic stress distribution, $\sigma_x = My/I$.
5. Calculate the shear stresses due to torsion, $\tau_{xy} = \frac{T}{2tA_o}$.
6. Assume $\sigma_y = 0$ (No out of plane bending is considered).
7. Calculate the ratios $\frac{\sigma_x}{|\tau_{xy}|}$ and $\frac{\sigma_y}{|\tau_{xy}|}$ for each region.
8. Select design equations as explained in the numerical example (Appendix A).
9. Calculate the required reinforcement.

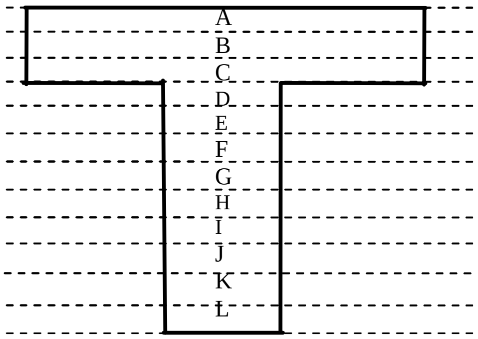
A
B
C
D
E
F
G
H
I
J
K
L

Figure 2. Regions (Levels) in the cross-section

The required reinforcement at mid-span was provided over a test span length of 1200mm in the middle of beam. Figure 3 shows typical reinforcement arrangements in a tested T-beam and Fig. 4 shows details of provided reinforcement in the test span of each beam. The solid dots in the figure indicate the locations of bars, which were strain-gauged.

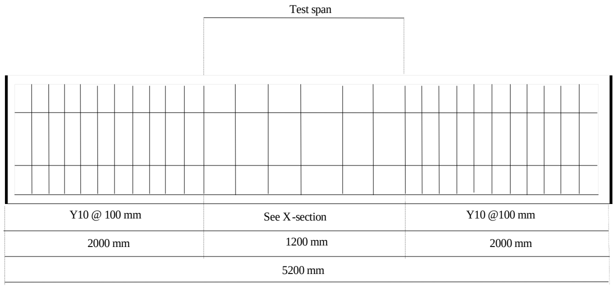
Test span
Y10 @ 100 mm
See X-section
Y10 @100 mm
2000 mm
1200 mm
2000 mm
5200 mm

Figure 3. Typical arrangement of reinforcement

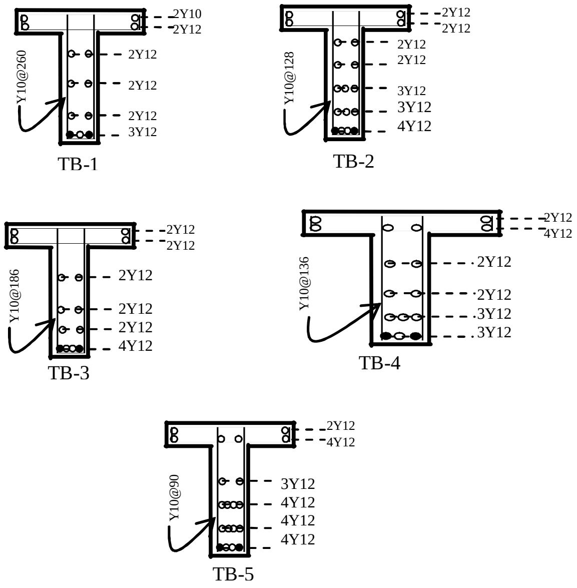
2Y10
2Y12
2Y12
2Y12
2Y12
3Y12
Y10@260
TB-1
2Y12
2Y12
2Y12
2Y12
3Y12
3Y12
4Y12
Y10@128
TB-2
2Y12
2Y12
2Y12
2Y12
2Y12
4Y12
Y10@186
TB-3
2Y12
4Y12
2Y12
2Y12
3Y12
3Y12
Y10@136
TB-4
2Y12
4Y12
3Y12
4Y12
4Y12
4Y12
Y10@90
TB-5

Figure 4. Provided reinforcement at test span

To ensure failure at mid-span, additional reinforcement was provided in the regions outside the test span. Further, to reduce the stresses due to distortion of the cross section and produce good griping mechanism in the torsional arms, the end section was made 600x600 mm solid square for a length of 400mm from each end.

6. Casting of Beams

After the steel cage was erected including all longitudinal and transverse reinforcement, the beam was cast in a specially designed wooden and Glass Reinforced Plastic (GRP) formwork. One day after casting, the sides of the mould were disassembled leaving the bottom part bellow the beam. Six concrete cubes (100mm) and six cylinders (150 x 300mm) were cast with each beam from the concrete used in the beam. A vibrating table was used for compaction of the cubes and cylinders while the beam was vibrated using an external vibrator attached to the shuttering. The beam and the cubes and cylinders were cured using wet Hessian cloth for about one week and then in room temperature for another three weeks. All cubes and cylinders were tested on the day the beam was tested to determine the cube and cylinder compressive strengths and cylinder tensile strength. Only 10mm and 12mm High Yield steel bars were used as longitudinal reinforcement and 10mm bars were used for stirrups. From the tensile test results, the average yield stress of steel was 545N/mm^2 for longitudinal reinforcement and 513N/mm^2 for stirrups. Ordinary Portland cement (OPC), fine aggregate, coarse aggregate (10mm) and fresh water were used in the concrete mix. Table 3 shows the average of some measured material properties.

Table 3. Measured average material properties

Beam No.	f_{cu} N/mm^2	f_y N/mm^2	f_{yv} N/mm^2
TB1	36	500	500
TB2	30	596	515
TB3	45	500	500
TB4	29	565	525
TB5	30	565	525

7. Experimental Set-up

Figure 5 shows the testing rig with a typical beam installed. The installation process required inserting the beam square ends into the torsional arms (Fig. 6) which are attached to shafts and bearings resting on pedestals (Fig. 7). The torsional arm ends are hooked to the strong floor by inextensible cables with hydraulic actuators and load cells. On the top face of the beam, a 1200mm long spreader was installed. The spreader was centred at the mid-span of the beam with its centreline coinciding with beam centreline. The bending moment in the middle 1200mm test span is acquired by applying a point load at the middle of the spreader. The torsional moment which is constant over the entire length of the beam, was applied through torsional arms clamped at the ends. The load from the spreader was transferred to the beam through two perpendicular rollers in one side while a roller and a pin were installed at the other side. This support and loading arrangements produced a simply supported condition allowing free rotation about the longitudinal axis of the beam and horizontal displacements with a rigid body motion being prevented by the pin on the top face. The test span region is mainly subjected to bending and twisting moments while outside the test span shear is added to the twisting and bending moments.

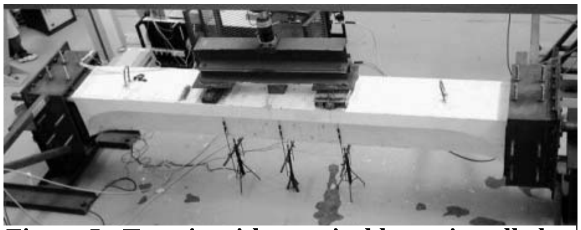

Figure 5. Test rig with a typical beam installed

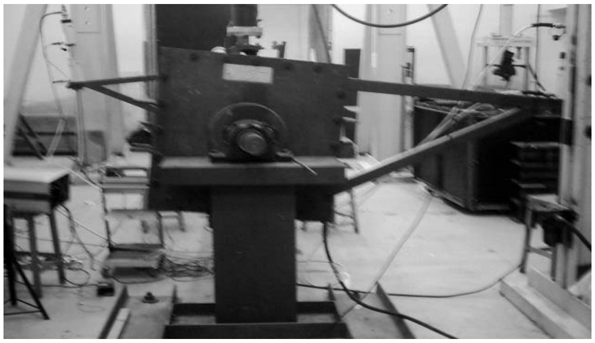

Figure 6. Torsional arm while testing

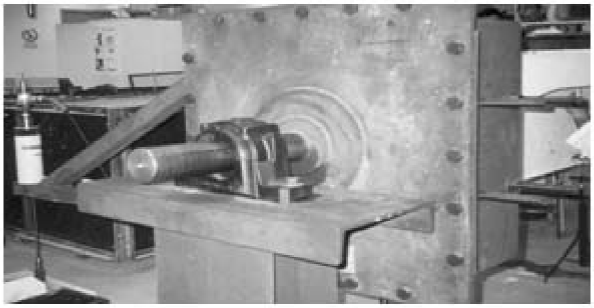

Figure 7. Close lookup of end support and torsional arm with actuator and load cell

Strains in the reinforcement were monitored using electrical resistance strain gauges. Figure 8 shows the legend

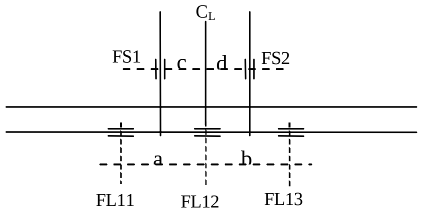

(a) Front side

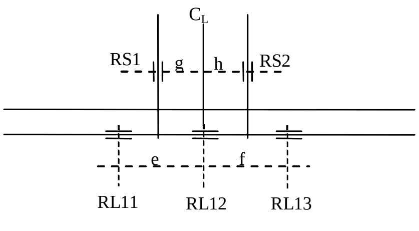

(b) Rear side

Figure 8. Legend for strain gauge locations in longitudinal and transverse steel (see Table 4)

Table 4. Location of strain gauges (see Figure 8)

Space	**a**	**b**	**c**	**d**	**e**	**f**	**g**	**h**
Beam	mm	mm	mm	mm	mm	mm	mm	mm
TB1	260	260	130	130	260	260	130	130
TB2	128	128	64	64	128	128	64	64
TB3	186	186	93	93	186	186	93	93
TB4	136	136	68	68	136	136	68	68
TB5	90	90	45	45	90	90	45	45

Vertical dist. for the stirrup's strain gauges is 300mm from the bottom of the web.

Table 5. Vertical clear distances between longitudinal bars (see Fig. 9)

Location	**1**	**2**	**3**	**4**	**5**	**6**	**7**
Beam	mm	mm	mm	mm	mm	mm	mm
TB1	20	100	100	120	-	20	20
TB2	20	80	80	100	100	20	20
TB3	20	100	100	120	-	20	20
TB4	20	100	100	120	-	20	20
TB5	20	100	100	120	-	20	20

and arrangement of the strain gauges in the longitudinal and transverse reinforcement and Table 4 gives the location of strain gauges for each beam. At each specified location on each bar, two strain gauges were installed opposite to each other. Figure 9 shows typical locations of the longitudinal bars and Table 5 shows vertical distances between the longitudinal bars.

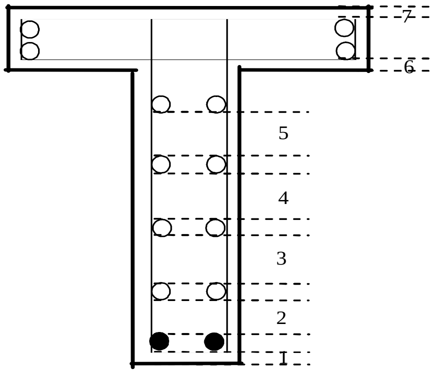

Figure 9. Typical vertical clear spaces between longitudinal bars (see Table 5)

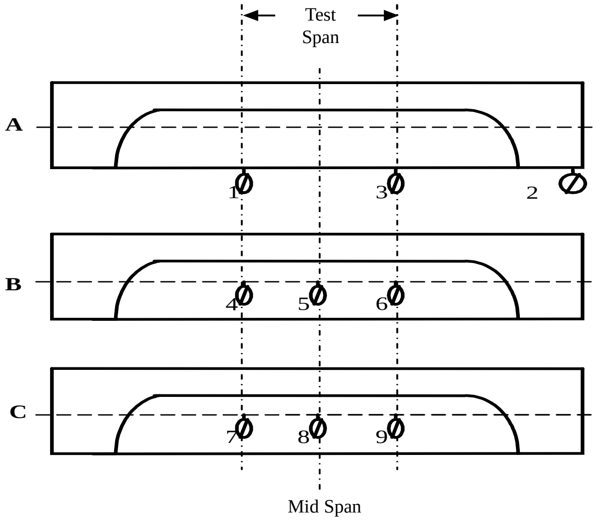

a: Bottom side transducers B: Front sdie transducers C: Rear side transducers

Figure 10. Locations of LVDT

Linear variable differential transducers (LVDT) were used to measure the beam deflection (Fig. 10). The concrete surface strains were measured by DEMEC (digital) gauges. All strain gauges and LVDTs were hooked to a data logger. The crack widths were measured using a crack width measuring microscope.

For each experiment, the design load was divided into load increments, 10% of the design load for each of the first three increments and 5% for each of the following increments until failure. The first step was to zero all load cells and record instrument readings with minimum possible loads on the model. Flexural loads were normally applied before torsional load at each load level. To allow for stable deformation to take place after each load increment, an interval of about two minutes was used before recording the instrument readings. After the steel strains and displacement readings were recorded, cracks were marked and DEMEC readings were taken before the next load was applied. The beam was considered to have collapsed when it could resist no more loads. This usually happened after a major crack spiralled around the beam near the mid-span dividing the beam into two parts connected by the longitudinal reinforcement.

8. Experimental Observations

This section summaries the observed behaviour in the test span region of the tested T-beams at significant stages in the behaviour. The angle of crack was measured from the horizontal axis. Vertical displacement was measured at the mid-span at the bottom of the web. Strain ratios in the bottom layer of the longitudinal steel and in the transverse steel of mid-span are presented. The quoted load factor is a percentage of the experimentally measured load at each increment to the design load, L.F. = $(M_i/M_d + T_i/T_d)/2$ including the self-weight. The failure load is a percentage of the experimentally measured failure load to the design load, $L_e/L_d = (M_e/M_d + T_e/T_d)/2$.

The average strain ratio in the longitudinal $\varepsilon/\varepsilon_y$ or transverse $\varepsilon/\varepsilon_{yv}$ reinforcements is the average of the measured strain at each load increment to the yield strain. At each strain-gauge location on the bar, the average of the readings from the two opposite strain gauges is considered.

$$\text{TB1: } T_d=36\text{kNm},\ M_d=60\text{kNm},\ T_d/M_d=0.6 \qquad (1)$$

The first few cracks were noticed at 45% of load at the bottom of the web near mid-span. The cracks were about 80o inclined. More cracks developed by the increase of the load until about 90% of the design load with angle of inclination being reduced to an average of 50^o and average width of crack of about 0.4 mm. After this stage, few major inclined cracks started out side the test span. Near failure, prominent cracks spiralled round the beam meeting near the mid-span. The failure happened at 110% of the design load. The average crack width just before failure was about 0.6 mm. Figure 11 shows the displacement at mid-span of the beam and Figs. 12-15 show strain ratios in the longitudinal and transverse reinforcement. The average strain ratio reached near failure in the longitudinal steel was 0.94 and in the stirrups, the ratio was 0.92. Figure 16 shows crack development in the test-span of the beam.

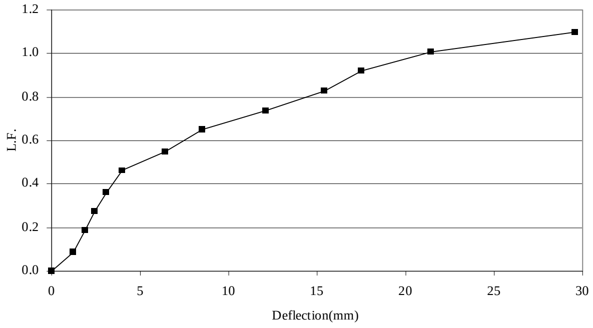

Figure 11. Deflection at mid-span (TB1)

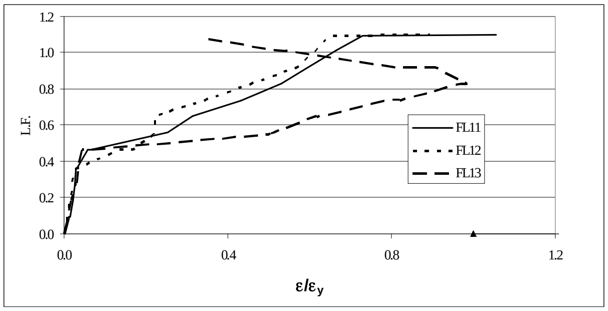

Figure 12. Front side longitudinal steel strain ratios (TB1)

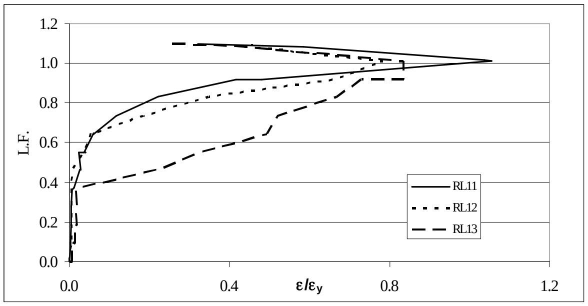

Figure 13. Rear side longitudinal steel strain ratios (TB1)

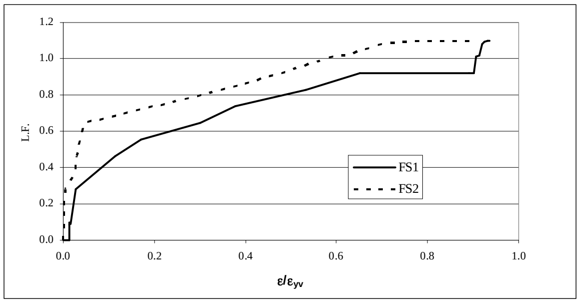

Figure 14. Front side transverse steel strain ratios (TB1)

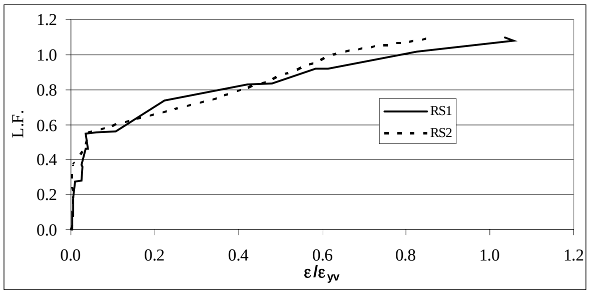

Figure 15. Rear side transverse steel strain ratios (TB1)

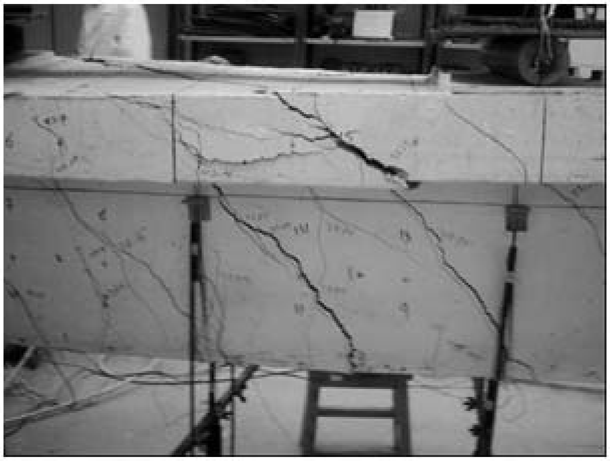

Figure 16. Crack development (TB1)

$$\text{TB2: } T_d=75\text{kNm},\ M_d=100\text{kNm},\ T_d/M_d=0.75 \qquad (2)$$

At 40% of load, several inclined hair cracks (about 60^o) were noticed in the test span region close to the bottom of the web. With the increase of the load, many fine cracks developed until about 90% of load when two major cracks widened up (45^o inclination) and spiralled around the beam causing failure at 105% of the design load. The average crack width near failure load was about 0.5 mm.

Figure 17 shows the displacement at mid-span and Figs. 18-19 show the strain ratios in the longitudinal and transverse bars. The average strain ratio in the longitudinal bars 0.9 and in the stirrups was 0.61. Figure 20 shows crack development in this beam.

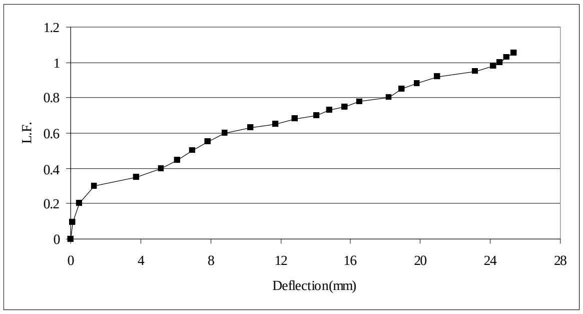

Figure 17. Deflection at midspan (TB2)

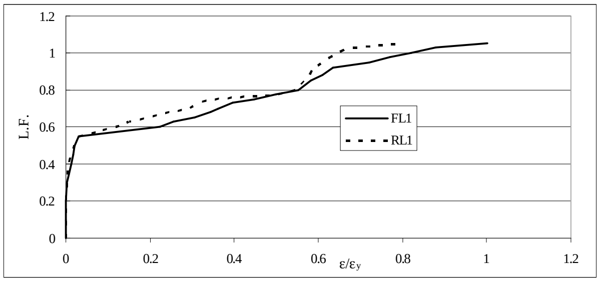

Figure 18. Longitudinal steel strain ratios (TB2)

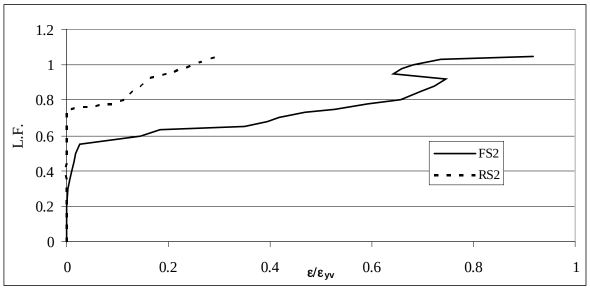

Figure 19. Transverse steel strain ratios (TB2)

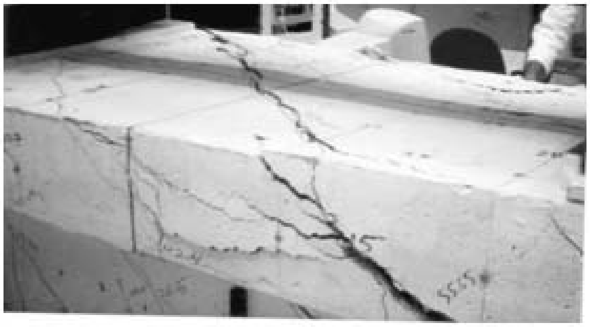

Figure 20. Crack development (TB-2)

TB3: T_d=50kNm, M_d=60kNm, T_d/M_d=0.83 (3)

The development of cracks in this beam was similar to that of beam TB2 with number of cracks being larger in TB3 than TB2. Failure happened at 112% of the design load. Figure 21 shows displacement at mid-span and Figs. 22-25 show steel strain ratios in the longitudinal and transverse steel. Figure 26 shows crack development in this beam. The average width of cracks near failure was 0.45 mm and the average strain ratio near failure was 0.91 in the longitudinal steel and 0.85 in the stirrups.

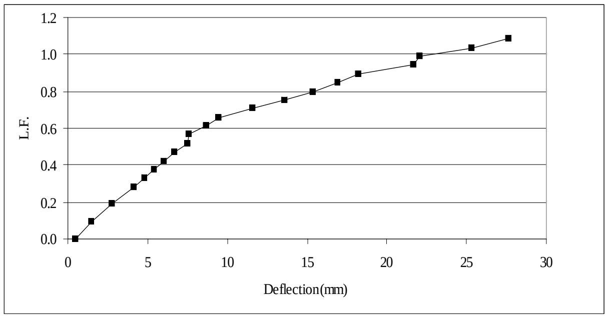

Figure 21. Deflection at midspan (TB3)

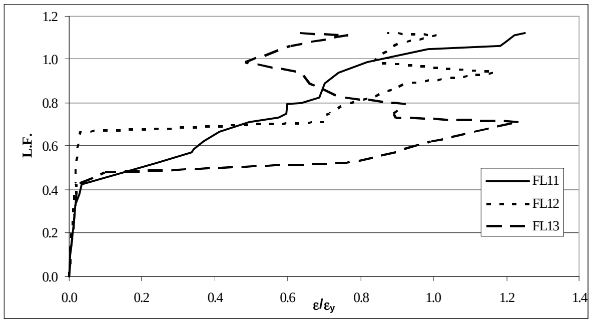

Figure 22. Front side longitudinal steel strain ratios (TB3)

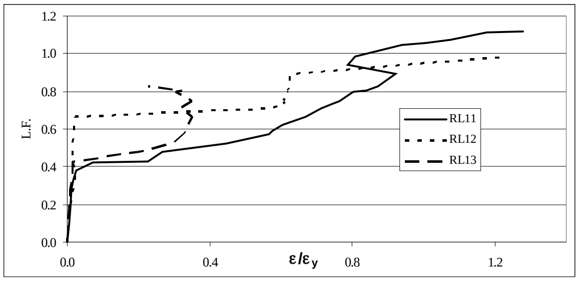

Figure 23. Rear side longitudinal steel strain ratios (TB3)

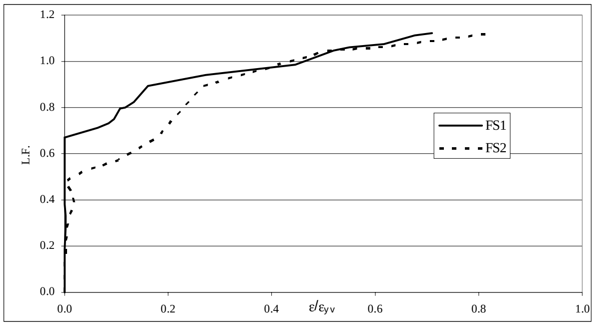

Figure 24. Front side transverse steel strain ratios (TB3)

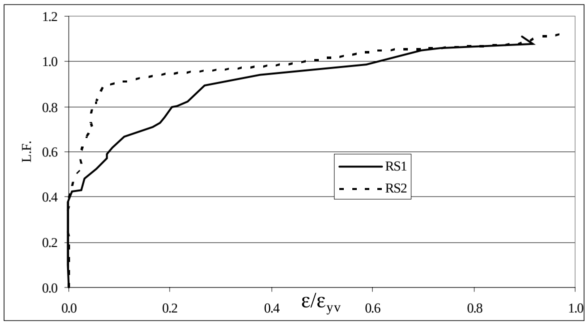

Figure 25. Rear side transverse steel strain ratios (TB3)

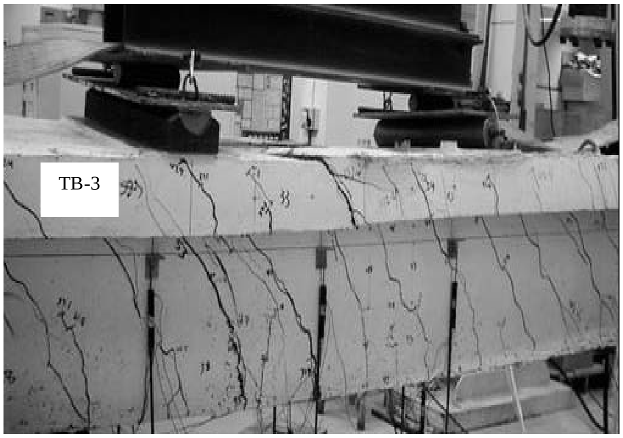

Figure 26. Crack development (TB3)

TB4: T_d=72kNm, M_d=72kNm, T_d/M_d=1.0 (4)

At 25% of load, few inclined cracks (about 45°) started in the lower part of the web. The number of cracks increased largely with the increase of the load but the width was smaller than in the previous beams. The beam failed at 100% of the design load with few cracks widened slightly larger than the others did. Figure 27 shows displacement at mid-span and Figs. 28-31 show steel strain ratios in the longitudinal and transverse steel. Figure 32 shows crack development in this beam. The average width of cracks near failure was 0.4 mm and the average strain ratio near failure was 1.05 in the longitudinal steel and 0.94 in the stirrups.

TB5: T_d=108kNm, M_d=72kNm, T_d/M_d=1.5 (5)

This beam behaved in a similar manner like TB4 but

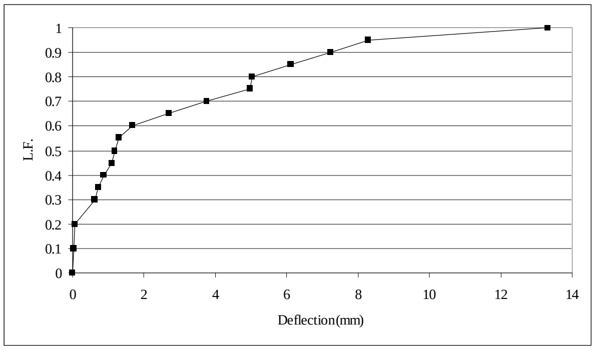

Figure 27. Deflection at midspan (TB4)

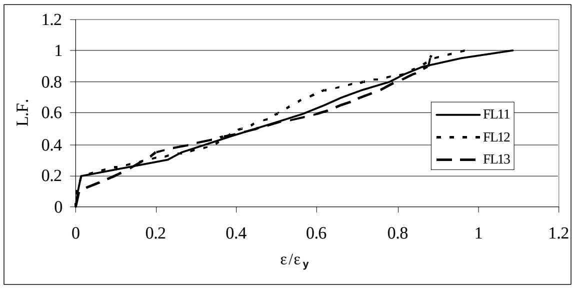

Figure 28. Front side longitudinal steel strain ratios (TB4)

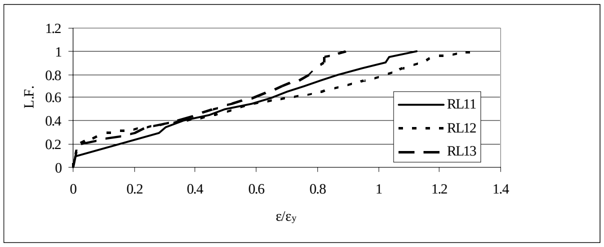

Figure 29. Rear side longitudinal steel strain ratios (TB4)

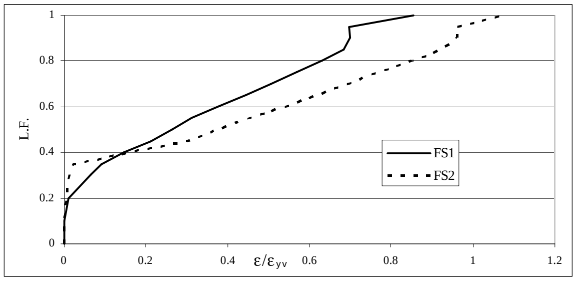

Figure 30. Front side transverse steel strain ratios (TB4)

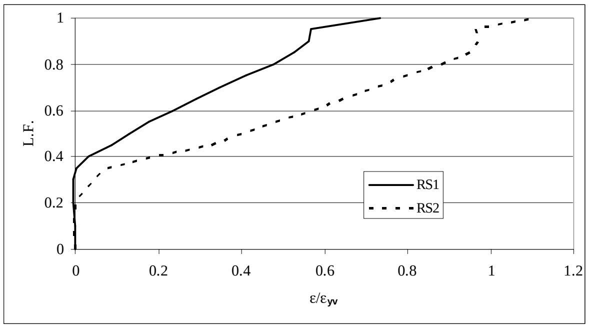

Figure 31. Rear side transverse steel strain ratios (TB4)

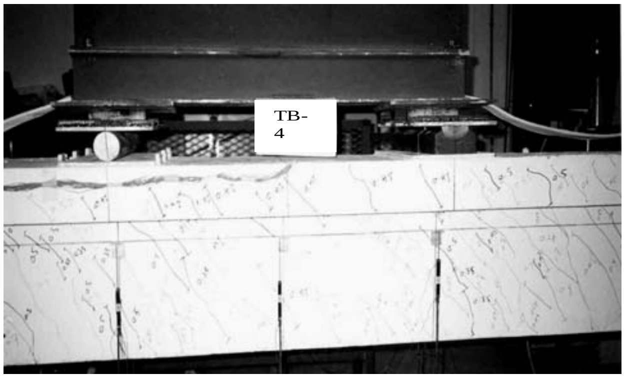

Figure 32. Crack development (TB4)

with larger number and finer cracks. There was no major cracks but the beam failed by losing strength due to the large number of cracks at a load of 98% of the design load. Figure 33 shows displacement at mid-span and Figs. 34-35 show steel strain ratios in the longitudinal and transverse steel. Figure 36 shows crack development in this beam. The average width of cracks near failure was 0.3 mm and the average strain ratio near failure was 1.04 in the longitudinal steel and 0.92 in the stirrups.

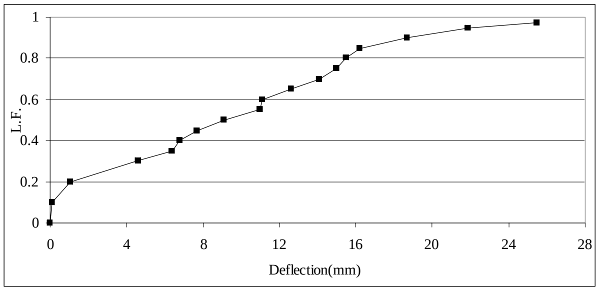

Figure 33. Deflection of midspan (TB5)

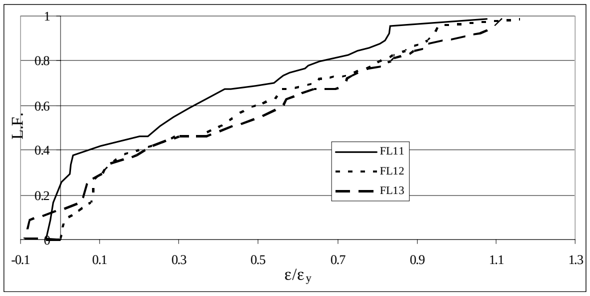

Figure 34. Front side longitudinal steel strain ratios (TB5)

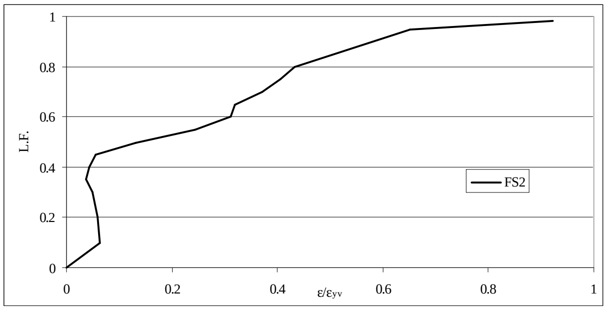

Figure 35. Front side transverse steel strain ratios (TB5)

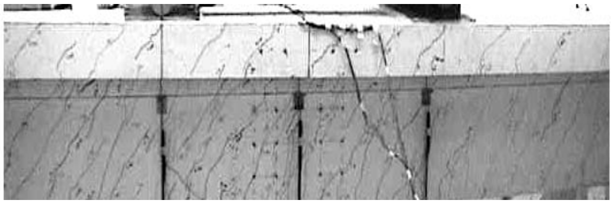

Figure 36. Crack development (TB5)

9. Discussion of Results

In all beams, the longitudinal and transverse steel either yielded or reached nearly the yield strain. This is to be expected since the beams were designed according to the lower bound theory of plasticity. Beams loaded dominantly in bending (*ie*. low T_d/M_d ratio) showed more ductile behaviour than those with large T_d/M_d ratios (Table 7). In general, all beams showed ductile behaviour as expected for under-reinforced sections. Furthermore, there was no crushing of concrete before yielding of steel. All beams failed near their design loads for all variations of T_d/M_d ratios (Column 3 of Table 6).

Table 6. Experimental/design failure load ratios

Load Beam	T_d/M_d Ratio	L_e/L_d Ratio
TB1	0.60	1.1
TB2	0.75	1.05
TB3	0.83	1.12
TB4	1.00	1.00
TB5	1.50	0.98
	Average	1.05

Table 7. Load-crack and displacement measurement

Beam No.	Load at first crack	Average max. Crack width near failure	Max. Disp. Near failure
	Ratio	mm	mm
TB1	0.45	0.6	29.6
TB2	0.4	0.5	25.3
TB3	0.4	0.45	27.6
TB4	0.25	0.4	13.3
TB5	0.25	0.3	25.5
Average	0.35	0.39	24.26

Beams loaded dominantly in bending (T_d/M_d <1) had vertical cracks started to develop first at the bottom of the web, then progressed as inclined cracks in succeeding load increments until reaching the flange at about 80% of the design load.

Beams loaded dominantly in torsion (T_d/M_d >1) had inclined cracks started at mid-depth in the web before they extend into the bottom of the web. Generally, cracks formed earlier in beams loaded dominantly in torsion (T_d/M_d >1) than other beams. In these beams, cracking started at a load as early as 25% of design load, while in other beams, they started at about 40% of design.

In beams where bending was dominant, the cracks in the test span were less in number and wider than in the beams where torsion was dominant. This is due to the fact that torsion was constant throughout the entire length while maximum bending moment existed over a small distance at the middle of the beam.

10. Conclusions

From the results shown in this paper, it can be concluded that the direct design method produces a safe design for reinforced concrete T-beams under combined loading of bending and torsion. Most of the beams failed near design loads and undergone ductile behaviour until failure. The reinforcement yielded or reached near yield when the design load was approached. The direct design method required less longitudinal reinforcement than the BSI code and close to the reinforcement required by the ACI code. It required less transverse reinforcement than both BSI and ACI codes.

References

Abdel-Hafez Laila, M., 1986, "Direct Design of Reinforced Concrete Skew Slab," PhD Thesis, University of Glasgow, 1986.

ACI committee 318, "Building Code Requirements for structural Concrete (ACI318M-02) and Commentary (ACI318RM-02)," American Concrete Institute, Farmington Hills, Mich. 48333-9094, USA.

Ali Alnuaimi and Bhatt, P., 2004a, "Direct Design of Hollow Reinforced Concrete Beams -Part I: Design Procedure," *Structural Concrete Journal*, Vol. 5(4), pp. 139-146.

Ali Alnuaimi and Bhatt. P., 2004b, "Direct Design of Hollow Reinforced Concrete Beams -Part II: Experimental Investigation," *Structural Concrete Journal*, Vol. 5(4), pp. 147-160.

Bhatt, P. and Bensalem, A., 1996a, "Behaviour of Reinforced Concrete Flat Slab Over Column Support using Nonlinear Stress Field Design," Structural Engineering Review, Vol. 8(2-3), pp. 201 - 212.

Bhatt, P. and Bensalem, A., 1996b, "Use of Non-elastic Stress in the Design of Reinforced Concrete Deep Beams," Structural Engineering Review, Vol.8(2-3), pp. 213 - 225.

Bhatt, P. and Ebireri, J. O., 1989, “Direct Design of Beams for Combined Bending and Torsion,” Stavebnicky Casopis, Vol. 37(4), pp. 249-263.

Bhatt, P. and Mousa, J., 1996, "Tests on Concrete Box Beams under Non-monotonic Loading," Structural Engineering Review, Vol. 8(2-3), pp. 227 - 235.

BS8110, 1997, "Structural Use of Concrete, Part1: Code of Practice for Design and Construction", British Standard Institution, 389Chiswick High Road, London, W4 4AL.

Elarabi, H., 1999, "Application of the Direct Design Method on Reinforced Concrete Beams subjected to Combined Torsion, Bending and Shear," *Building and Road Research Journal*, University of Khartom, Vol. 2, pp. 47-56.

El-Hussein, E. A., 1994, "Finite Element and Direct Design Method in Combined Torsion, Bending and Shear of Reinforced Concrete," Computational Structural Engineering for Practice,” Civil-Comp Ltd, Edinburgh, Scotland, pp. 165-171.

El-Nuonu, G. F. R., 1985, "Design of Shear Wall-floor Slab Connections," PhD Thesis, University of Glasgow, UK.

Farmer, L. E. and Ferguson, P. M., 1967, "Shear and Torsion", *ACI Journal*, pp. 757-65.

Gurfinkel, G. and Fonseca, F., 1996, "Designing T-Beams for less Ductility than required by ACI", *ACI Structural Journal*, Vol. 93(S12), pp. 116-127.

Hago, A. and Bhatt P., 1986, "Tests on Reinforced Concrete Slabs Designed by Direct Design Procedure," *ACI Journal*, Vol. 83-79(6), No.6, Nov.-Dec., 1986, pp. 916-924.

Kemp, K. O., 1971, "Optimum Reinforcement in a Concrete Slab Subjected to Multiple Loadings," *Publications of the International Association of Bridge and Structural Engineering*, pp. 93 - 105.

Kirk, D. W. and Loveland, N. C., 1972, "Unsymmetrically Reinforced T-Beams Subject to Combined Bending and Torsion," Paper No. 69-44, *ACI Journal*, pp. 492-99.

Kotsovos, M. D., Bobrowski, J., and Eibl, J., 1987, "Behaviour of Reinforced Concrete T-beams in Shear," The Structural Engineer, Vol. 65B(1), pp. 1-10.

Memon, M., 1984, "Strength and Stiffness of Shear Wall-floor Slab Connections," PhD Thesis, University of Glasgow, UK.

Morley, C. T. and Gulvanessian, H., 1977, "Optimum Reinforcement of Concrete Slab Elements", Proc. Institution of Civil Engineers, Vol. 63(2), pp. 441-454.

Nawy, E. G. and Potyondy, J. G., 1971, "Flexural Cracking Behaviour of Pretensioned I- and T-Beams,” *ACI Journal*, pp. 355-360

Nielsen, M. P., 1974, Optimum Design of Reinforced Concrete Shells and Slabs,” Structural Research Laboratory, Technical University of Denmark, Report NR.R44, pp.190-200.

Rahal, K. N. and Collins, M. P., 2003, "Experimental Evaluation of ACI and AASHTO-LFRD Design Provisions for Combined Shear and Torsion," *ACI Structural Journal*, Vol. 100(3), pp. 277 - 282.

Zararis, P. D. and Penelis, G. Gr., 1986, "Reinforced Concrete T-beams in Torsion and Bending," *ACI Journal*, Title No. 83-17, pp. 145-55.

Appendix

Example: Design of T-beams using Direct Design Method

TB3: **T_d=50 kN.m** **M_d=60 kN.m** **T_d/M_d =0.83**

See Figs: 1 and 2.

- Gross-sectional area (Fig. A1):

A=600x150+200x450=180000mm^2

- Depth of neutral axis from top of flange:

600x150x150/2 + 200x450x375= (600x150+200x450) $\overline{x}$

$\overline{x}$ = 225mm

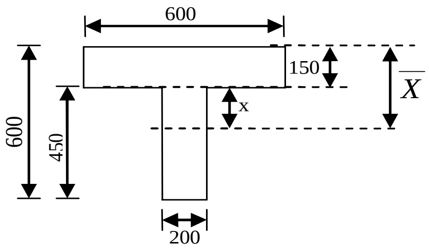

Fig. A1: Geometry of cross-section

For torsion assume 50mm effective wall thickness (Fig. A2):

- Area of section within the shear flow centerline,

A_o = 100x550 + 150x425 = 11.875x 10^4 mm^2

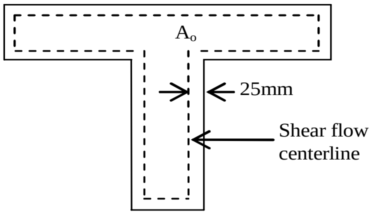

Fig. A2: Shear flow centerline

- Moment of inertia, I = $\frac{1}{3}$[600x225^2+200(600-225)^3-75^3(600-200)] =5.7375x10^{4}mm^4
- Normal stress due to bending at the centroid of each level: $\sigma_i = \frac{My_i}{I}$, *i* = level reference and y=distance between level centroid and neutral axis (Column 3 of Table A1).
- Assume ó$_{yi}$ = 0, No out of plane bending (Column 4 of Table A1).

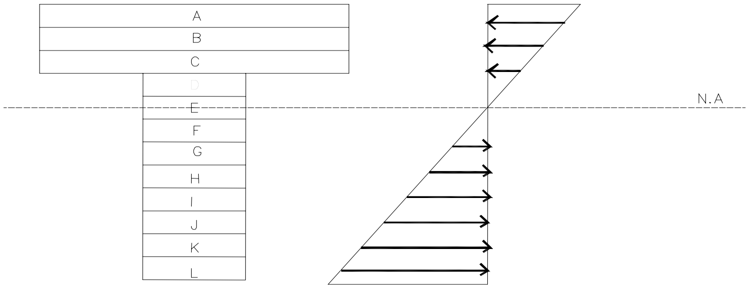

Fig. A3: Levels (regions) in the cross section and normal stress.

- Calculate shear stress due to torsion, wall thickness 50mm (Column 5 of Table A1):

$$\tau_{xy} = \frac{T}{2tA_o} = \frac{50x10^6}{2x50x11.875x10^4} = 4.21N / mm^2$$

- Calculate ó$_{xi}$ / ô$_{xy}$ and ó$_{yi}$ / ô$_{xy}$ (columns 6 and 7 of Table A1).
- Select the design case from the boundary graph for Nielsen's design equations shown in Fig. A4 (Column 8 of Table A1).
- Calculate forces in the longitudinal direction per unit length: $N_x^s = N_x + \left|N_{xy}\right|$ (Column 9 of Table A1).
- Calculate forces in the transverse direction per unit length: $N_y^s = N_y + \left|N_{xy}\right|$ (Column 10 of Table A1).
- Calculate steel areas for each region in the x and y directions, assume f_y = f_{yv} = 500N/mm^2 (columns 11 and 12).
- Select the number of bars and bar size based on the available sizes and required areas.
- Detail calculation for level A is shown below Table A1.

Table A1: Calculation of reinforcement for Example A

1 Level	2 Width (mm)	3 ó$_{xi}$ (N/mm^2)	4 ó$_{yi}$ (N/mm^2)	5 ô$_{xy}$ (N/mm^2)	6 ó$_{xi}$ / ô$_{xy}$	7 ó$_{yi}$ / ô$_{xy}$	8 Case	9 N_x^s (N /mm)	10 N_y^s (N /mm)	11 A$_{sx}$ (mm^2)	12 A$_{sy}$ (mm^2 /m)
A	600	-2.09	0	4.21	-0.496	0	3	106	210	127.2	420
B	600	-1.57	0	4.21	-0.373	0	3	132	210	158.4	420
C	600	-1.05	0	4.21	-0.249	0	3	158	210	189.6	420
D	200	-0.52	0	4.21	-0.124	0	3	184.5	210	73.8	420
E	200	0	0	4.21	0	0	3	210	210	84	420
F	200	0.52	0	4.21	0.124	0	3	236.5	210	94.6	420
G	200	1.05	0	4.21	0.249	0	3	263	210	105.2	420
H	200	1.57	0	4.21	0.373	0	3	289	210	115.6	420
I	200	2.09	0	4.21	0.496	0	3	315	210	126	420
J	200	2.61	0	4.21	0.62	0	3	341	210	136.4	420
K	200	3.14	0	4.21	0.746	0	3	367.5	210	147	420
L	200	3.66	0	4.21	0.869	0	3	393.5	210	157.4	420

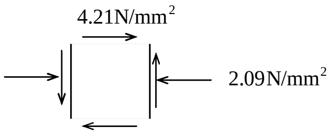

Detail Calculation for level A:

Col. 3: $\sigma_A = \frac{-My_A}{I} = \frac{-60x10^6x200}{5.7375x10^9} = -2.09N/mm^2$ (C)

Col. 8: From columns 6 & 7: we have: ó$_{xi}$ / ô$_{xy}$ = -0.496 and ó$_{yi}$ / ô$_{xy}$ = 0 ? from Fig A4 the location of this point lies in the region of case 3.

Col. 9: The force in x direction calculated as given in Fig. A 4: $N_x^s = N_x + |N_{xy}| = 50(-2.09+4.21) = 106\,N/mm$.

Col. 10: The force in y direction calculated as given in Fig. A 4:

$$N_y^s = N_y + |N_{xy}| = 50(0+4.21) = 210N/mm\,.$$

Col. 11: The steel area in x direction is given by: $A_x = \frac{N_x^s}{f_y} = \frac{106}{500} = 0.212mm^2/mm \Rightarrow = 0.212x600 = 127.2mm^2$.

Col. 12: The steel area in y direction is given by: $A_y = \frac{N_y^s}{f_{yv}} = \frac{210}{500} = 0.42mm^2/mm \Rightarrow = 0.42x1000 = 420mm^2/m$

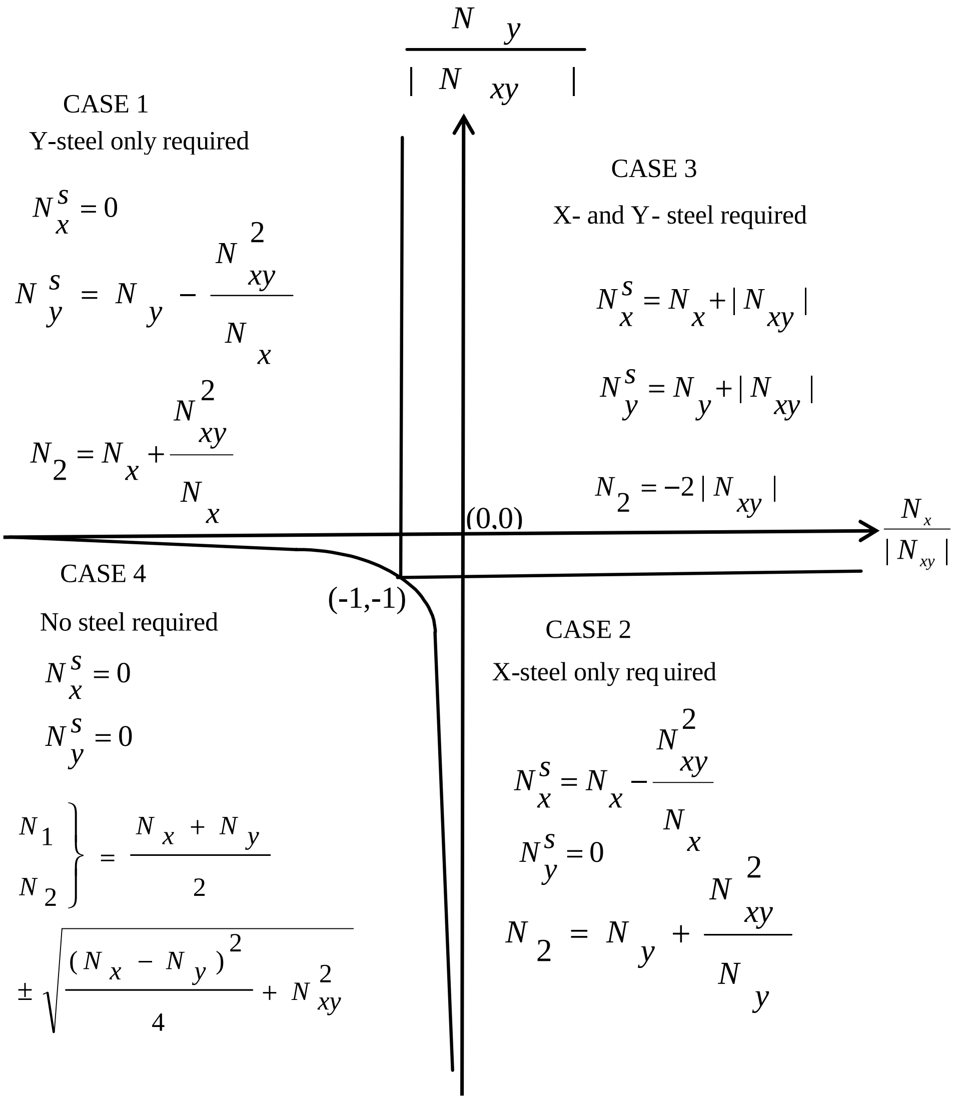
$\frac{N_y}{|N_{xy}|}$
CASE 1
Y-steel only required
$N_x^s = 0$
$N_y^s = N_y - \frac{N_{xy}^2}{N_x}$
$N_2 = N_x + \frac{N_{xy}^2}{N_x}$
CASE 3
X- and Y- steel required
$N_x^s = N_x + |N_{xy}|$
$N_y^s = N_y + |N_{xy}|$
$N_2 = -2|N_{xy}|$
(0,0)
$\frac{N_x}{|N_{xy}|}$
CASE 4
No steel required
$N_x^s = 0$
$N_y^s = 0$
$\left.\begin{matrix} N_1 \\ N_2 \end{matrix}\right\} = \frac{N_x + N_y}{2} \pm \sqrt{\frac{(N_x - N_y)^2}{4} + N_{xy}^2}$
(-1,-1)
CASE 2
X-steel only required
$N_x^s = N_x - \frac{N_{xy}^2}{N_x}$
$N_y^s = 0$
$N_2 = N_y + \frac{N_{xy}^2}{N_y}$

Fig. A4: Boundary graph for Nielson's 2D design equations